

# In<sub>2</sub>S<sub>3</sub>-TiO<sub>2</sub> heterojunction/electrospinning fiber composites for efficient photocatalytic hydrogen production

HAI FEI CHEN, JIE YANG\*, HAI QUN CHEN, YI HAO JIN, JING JING GUO, FU JIANG CHEN, NIANYONG ZHOU  
*School of Petroleum Engineering, Changzhou University, Changzhou, Jiangsu 213016, China*

An electrospun fiber with micro - nano - sized structure and carboxyl group was prepared by high - voltage electrospinning technology. In<sub>2</sub>S<sub>3</sub>-TiO<sub>2</sub> particles were formed on the surface of the electrospun fibers by the hydrothermal method. The In<sub>2</sub>S<sub>3</sub>-TiO<sub>2</sub> heterojunction/electrospinning fiber were characterized by SEM, XRD, XGA, TGA and UV-Vis. The In<sub>2</sub>S<sub>3</sub>-TiO<sub>2</sub> heterojunctions can be evenly distributed on electrospun fibers. The photocatalytic hydrogen production performance of the composites was studied by using xenon lamp in the visible light source. Na<sub>2</sub>S / Na<sub>2</sub>SO<sub>3</sub> was used as the sacrificial agent. The results show that the composite material has better photocatalytic hydrogen production capacity than the powder catalyst, and the average hydrogen production capacity is 15.29ml every two hours.

(Received June 8, 2017; accepted April 8, 2019)

*Keywords:* Polymer composites, Photocatalytic hydrogen production, Heterojunction

## 1. Introduction

Solar energy is the most abundant energy available on the earth. Renewable energy is the potential way to answer the needs of more energy [1-3]. In recent years, the application of semiconductor materials in photocatalytic hydrogen has become a hot topic for scholars all over the world [4, 5]. In order to find out efficient photocatalyst, many scholars have made a lot of research, and achieved good photocatalytic effect [6-8]. However, the powder photocatalyst still has some practical problems such as easy recombination of electron-hole pairs, small surface areas, poor dispersibility, easy floating sticky wall, and difficulty of recycling. The semiconductor was loaded on a specific carrier and In<sub>2</sub>S<sub>3</sub>-TiO<sub>2</sub> / electrospun fiber composites were prepared, which can improve the dispersion of the photocatalyst, increase the specific surface areas, and be readily recovered.

TiO<sub>2</sub> has been extensively studied for its excellent chemical stability in a variety of photocatalysts, such as non-toxicity, optical and electronic properties, and low cost [9-11]. However, TiO<sub>2</sub> absorbs ultraviolet light only due to its wide band gap of 3.2 eV. Since the UV region occupies only near 4% of the entire solar spectrum, while 45% of the energy belongs to visible light which most solar energy cannot be used. Thus, the development of efficient photocatalysts with visible-light response has become the focus of research [12-14].

In order to efficiently utilize solar energy, a number of attempts have been made to extend the photo-response of

TiO<sub>2</sub> to visible region, such as sensitizing with dyes or narrow band-gap semiconductors and doping with transition metal ions [13-15].

Indium sulfide (In<sub>2</sub>S<sub>3</sub>) is a typical chalcogenide with a narrow-band-gap of 2.0-2.2 eV, has attracted interest as a promising photocatalyst under visible-light irradiation for its high photosensitivity, stable chemical composition at ambient conditions, and low toxicity [15-18].

## 2. Experimental

### 2.1. Materials

N, N-dimethylacetamide (DMAC) was obtained from Shanghai Pilot Chemical Co., Ltd. Styrene-maleic anhydride coelectrospinning (SMA) was purchased from Shanghai SpecTek petrochemical high tech Co., Ltd. Polyvinylidene Fluoride (PVDF) was purchased from Shanghai 3F New Material Co., Ltd. Acetone was purchased from Dandong Zhongxing Chemical Plant. Titanyl sulfate was brought from Rugao Chemical Reagent Factory. Indium nitrate and thioacetamide were supplied from Sinopharm Shanghai Chemical Reagent Co., Ltd.

### 2.2. Characterization

The morphologies of the products were characterized by scanning electron microscopy (JSM-6490LV), which

was bought from JEOL Co., Ltd. ESCALAB 250 X-ray photoelectron spectroscopy bought from Thermo Electron Co., Ltd was applied to study the structure of composites. The thermo-gravimetric analysis (TG-209-F3) purchased from NETZSCH-Gerätebau GmbH was utilized to estimate the weight loss of composites. The crystal structure was detected through the X-ray diffraction (D/MAX2500V) bought from Rigaku Co., Ltd. Ultraviolet-visible (UV/Vis) absorption spectra was obtained on a Shimadzu-2550 spectrophotometer purchased from Shimadzu Co., Ltd at room temperature. The amount of hydrogen production was measured by gas chromatography (SP-6801), which was purchased from Shandong Lunan Ruihong Chemical Instrument Co., Ltd. Photocatalysis experiment was conducted by Multifunctional chemical reaction instrument (SGY-IB) bought from Nanjing East Branch Electric Equipment Co., Ltd.

### 2.3. Electrospinning of PVDF/SMA

A certain mass ratio of SMA and PVDF were weighed into a three-necked flask with stirring and N<sub>2</sub>, and then they were dissolved with acetone and DMAC as solvent to prepare a spinning solution with a certain concentration. PVDF/SMA was prepared by high voltage electrospinning device.

### 2.4. Preparation of In<sub>2</sub>S<sub>3</sub>-TiO<sub>2</sub> heterojunction/electrospinning fiber composites

The PVDF/SMA fiber mats were immersed in 50 mL titanium sulfate aqueous solution at room temperature for 24 h, enabling Ti<sup>4+</sup> and the carboxyl groups on the surface of the PVDF/SMA fibers were fully complexed. The fiber mats containing Ti<sup>4+</sup> were placed in a hydrothermal reaction kettle with the volume of 50 mL, and reacting for 14 h at 120 °C. After being cooled to room temperature, the fibers were ultrasonically shaken and rinsed three times. Afterwards, the fibers are dried for 12 h at 60 °C. The as-prepared fiber mats were immersed in indium nitrate aqueous solution for 24 h at room temperature. The

fiber mats containing In<sup>3+</sup> were placed in a hydrothermal reaction kettle with the volume of 50 mL, and then 25 mL, 0.25 mol L<sup>-1</sup> thioacetamide aqueous solution was added, reacting for 14h at 120 °C. After being cooled at room temperature, the reaction product was removed and washed by ultrasonic deionized water for three times. Finally, In<sub>2</sub>S<sub>3</sub>-TiO<sub>2</sub> heterojunction/electrospinning fiber composites were prepared after being dried in vacuum for 12h at 60°C. Also, the In<sub>2</sub>S<sub>3</sub>-TiO<sub>2</sub> powders were prepared by the same conditions.

### 2.5. Production of H<sub>2</sub>

250 mL of deionized water was measured in a photochemical reaction apparatus. The complex system of Na<sub>2</sub>S / Na<sub>2</sub>SO<sub>3</sub> (0.10mol / L Na<sub>2</sub>S, 0.32 mol / L Na<sub>2</sub>SO<sub>3</sub>) was used as the sacrificial agent in the photochemical reaction instrument. In order to allow the catalyst to better receive light, the electrospun fiber composites (including In<sub>2</sub>S<sub>3</sub>-TiO<sub>2</sub> heterojunction 0.15g) were spread in water. Under the same conditions, In<sub>2</sub>S<sub>3</sub>-TiO<sub>2</sub> powder (0.15g) was used for photocatalytic hydrogen production. A xenon lamp was used to simulate visible light as a light source. The hydrogen volume is quantified by the drainage method to collect the gas generated which was measured once every two hours. N<sub>2</sub> was used as the carrier gas and the collected gas was analyzed by a gas chromatograph.

## 3. Results

Fig. 1(a) showed the SEM image of TiO<sub>2</sub> heterojunction/electrospinning fiber composites produced by electrospinning, we can see that In<sub>2</sub>S<sub>3</sub>/electrospun fiber composites can be formed after the hydrothermal reaction, because fluorine fibers with carboxyl can complex zinc ions. Fig. 1(b) showed that many In<sub>2</sub>S<sub>3</sub>-TiO<sub>2</sub> particles grew on the surface of electrospinning fibers. As shown in the inset in Fig. 1(b), In<sub>2</sub>S<sub>3</sub>/electrospun fiber composites were immersed in zinc nitrate solution, there are numerous acicular In<sub>2</sub>S<sub>3</sub> particles after hydrothermal reaction. The In<sub>2</sub>S<sub>3</sub> particles on the surface distributed evenly.

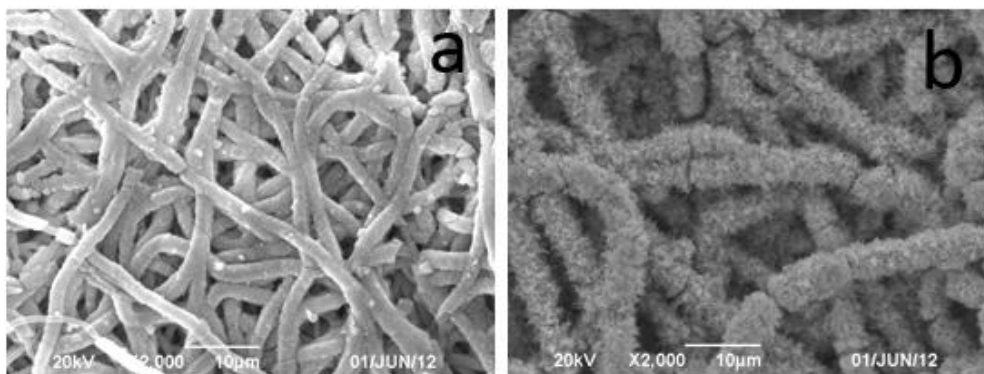


Fig. 1. SEM images of (a) TiO<sub>2</sub> heterojunction/ electrospinning fiber composites, and (b) In<sub>2</sub>S<sub>3</sub>-TiO<sub>2</sub> heterojunction/ electrospinning fiber composites

## 4. Discussions

### 4.1. Characterization of $\text{In}_2\text{S}_3\text{-TiO}_2$ heterojunction/electrospinning fiber composites

The phase structures of the  $\text{In}_2\text{S}_3\text{-TiO}_2$  heterojunction/electrospinning fiber composites and PVDF/SMA heterojunction/electrospinning fiber composites were investigated by XRD method and the results were shown in Fig. 2. In Fig. 2(a), the curve revealed that the crystal phase of  $\text{In}_2\text{S}_3$  was anatase with the diffraction peaks at about  $25.7^\circ$ ,  $37.8^\circ$ ,  $48.2^\circ$ ,  $53.8^\circ$  and  $64.2^\circ$ , which could be perfectly indexed to the (101), (004), (200), (105) and (211) crystal faces of  $\text{TiO}_2$  (PDF card 32 - 0456, JCPDS) respectively [19]. This proved that the  $\text{TiO}_2$  supported on the fibers were anatase structure, and the absorption peak of  $\text{TiO}_2$  was insignificant because  $\text{In}_2\text{S}_3$  cocooned  $\text{TiO}_2$ .

The composition and the valence state of the elements in  $\text{In}_2\text{S}_3\text{-TiO}_2$  heterojunction/electrospinning fiber composites were analyzed by XPS (Fig. 3a). The characteristic signals for C, O, F, S, In, and Ti are clearly detected in the composites, and the XPS spectra are exhibited in Fig. 4b-d. The S2p peak (Fig. 3b) is belong to the S-In bond at 161.78eV. The In 3d XPS curve of the composites (Fig. 3c) presents In 3d<sub>5/2</sub> at 444.98eV and In 3d<sub>3/2</sub> at 452.58eV. The 7.6 eV splitting of the In 3d doublet

indicated a normal state of  $\text{In}^{3+}$  in the prepared composites. The Ti 2p XPS curve of the composites (Fig. 4e) presented at 452.8 eV.

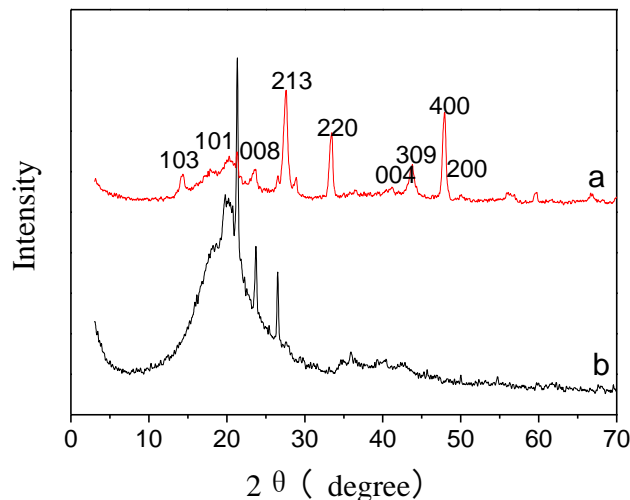


Fig. 2. The XRD patterns of (a)  $\text{In}_2\text{S}_3\text{-TiO}_2$  heterojunction/electrospinning fiber composites, and (b) PVDF/SMA heterojunction/electrospinning fiber composites

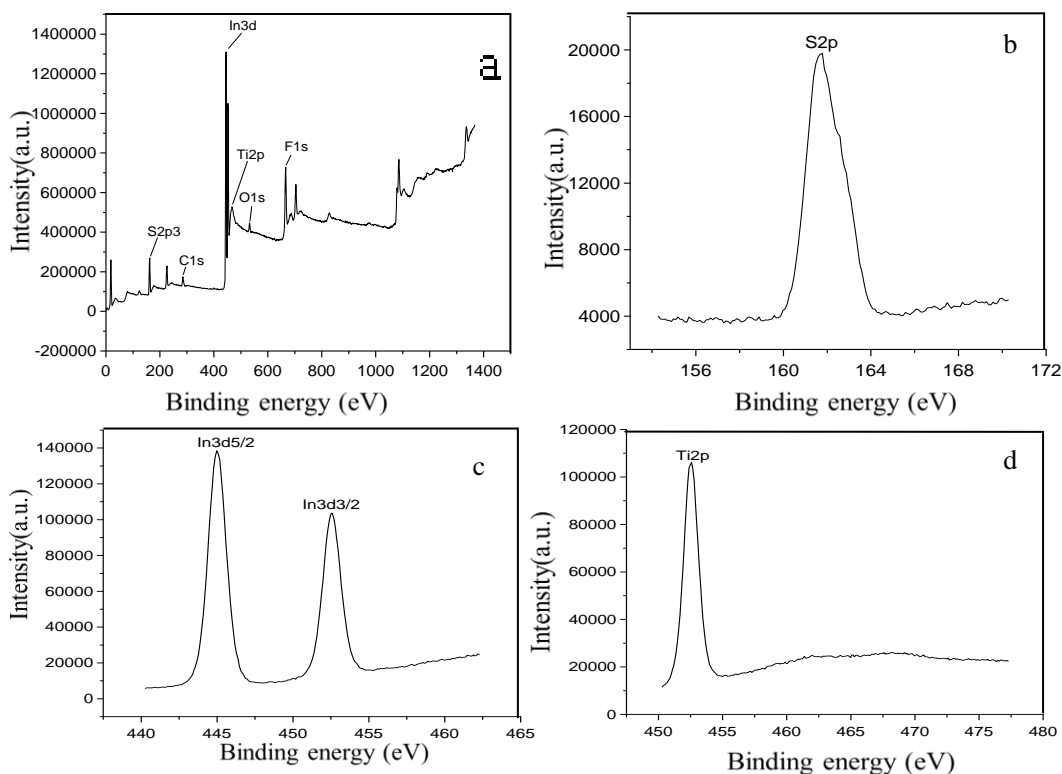


Fig. 3. XPS spectra of  $\text{In}_2\text{S}_3\text{-TiO}_2$  heterojunction/electrospinning fiber composites: (a) survey scan spectrum and high-resolution spectra of (b) S 2p, (c) In 3d, (d) Ti 2p

In Fig. 4 (a), the unsupported electrospinning fibers have no evident absorption between 250 and 800 nm, while composites have absorption peak sat round 630 nm, and the Xe lamp has a wavelength in the range of 320 to 800 nm. This reveals that the unsupported fibers do not interfere with the light absorption during the photocatalytic reaction. Fig. 4 (b) shows the absorption peak of In<sub>2</sub>S<sub>3</sub>-TiO<sub>2</sub>/electrospinning fiber composites sat round 630 nm, which indicates red shift occurred, because of the quantum effect.

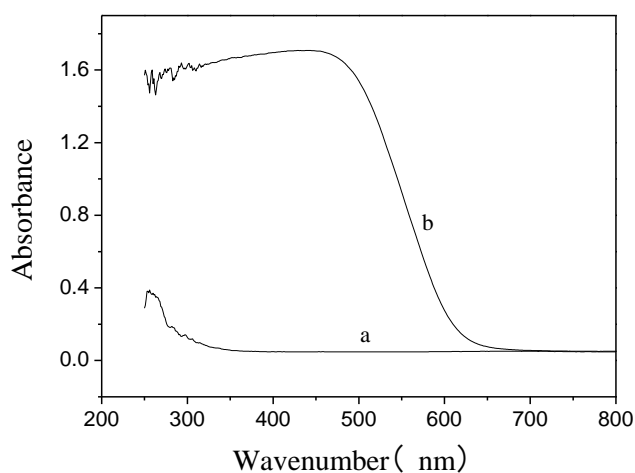


Fig. 4. UV-Vis absorption spectra of (a) PVDF/SMA electrospinning fiber and (b) In<sub>2</sub>S<sub>3</sub>-TiO<sub>2</sub> heterojunction/electrospinning fiber composites

#### 4.2. Photocatalytic H<sub>2</sub> evolution

Fig. 5 summarized H<sub>2</sub> evolution from splitting of water under Xe lamp irradiation using In<sub>2</sub>S<sub>3</sub>-TiO<sub>2</sub> heterojunction/electrospinning fiber composites and In<sub>2</sub>S<sub>3</sub>-TiO<sub>2</sub> powders as photocatalysts, respectively. The experiments were operated for three runs, with the aqueous solution of 0.1 mol L<sup>-1</sup> Na<sub>2</sub>S (1.95g) and 0.32 mol L<sup>-1</sup> Na<sub>2</sub>SO<sub>3</sub> (10.08g) as sacrificial agent. For every run, the reaction time kept 20 h, and the concentration of sacrificial agents was also identical. From the first to the third run, the amount of hydrogen produced by the In<sub>2</sub>S<sub>3</sub>-TiO<sub>2</sub> powders is almost constant. While under the same conditions, the hydrogen production of In<sub>2</sub>S<sub>3</sub>-TiO<sub>2</sub> electrospun fiber composites is obviously increased, which indicates that the catalyst has good recycle stability. And the amount of hydrogen produced by the composites in the third run is 1.49 times of In<sub>2</sub>S<sub>3</sub>-TiO<sub>2</sub> heterojunction powders, this is due to the large specific surface area of In<sub>2</sub>S<sub>3</sub>-TiO<sub>2</sub> supported by the electrospun fibers, and high utilization of the light source. Also, the hydrogen production rate of the In<sub>2</sub>S<sub>3</sub>-TiO<sub>2</sub> powders decreased obviously from 12h, while the hydrogen production rate of the composite materials remained basically unchanged,

which indicated that the composite materials had higher utilization efficiency of the sacrificial agent due to its larger specific surface area. Fan studied the reason for the increase of hydrogen production rate, and found that the interaction between the organic and inorganic phases increased as the reaction proceeding, and the hydrogen production rate increased.

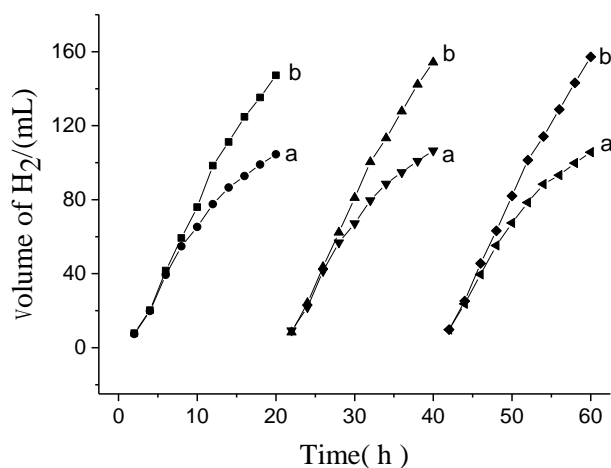


Fig. 5. Photocatalytic H<sub>2</sub> evolution of (a) In<sub>2</sub>S<sub>3</sub>-TiO<sub>2</sub> heterojunction/electrospinning fiber composites, and (b) In<sub>2</sub>S<sub>3</sub>-TiO<sub>2</sub> powders

#### 5. Conclusions

The In<sub>2</sub>S<sub>3</sub>-TiO<sub>2</sub> / electrospinning fiber composites were uniformly supported on the surface of the flanged electrospinning fibers by hydrothermal synthesis. The UV-Vis absorption spectra of In<sub>2</sub>S<sub>3</sub>-TiO<sub>2</sub> / electrospinning fiber composites show that the materials have good absorption under visible light, and electrospinning fiber absorption peak in the xenon lamp simulated sunlight catalytic hydrogen water does not affect the light absorption of the composite. In the process of photocatalytic hydrogen production, In<sub>2</sub>S<sub>3</sub>-TiO<sub>2</sub> / electrospinning fiber composite material has higher stability and activity relative to the powder catalyst, and the average hydrogen production capacity is 15.29 ml every two hours.

#### Acknowledgements

This work is supported by the Natural Science Foundation of Jiangsu Educational committee (No. 18KJD480001) and No. YZGX YJS2018-KYCX-012.

#### References

- [1] T. Y. Wei, K. L. Lim, Y. S. Tseng, S. L. I. Chan,

- Renew. Sust. Energ. Rev. **79**, 1122 (2017).
- [2] J. D. Holladay, J. Hu, D. L. King, Y. Wang, Catal. Today **139**(4), 244 (2009).
- [3] H. Chen, J. Ji, G. Pei, J. Yang, Y. Zhang, J. Clean. Prod. **174**, 1288 (2018).
- [4] A. K. Maparu, V. Ganvir, B. Rai, Colloids Surf. Physicochem. Eng. Aspects **482**, 345 (2015).
- [5] S. Verhelst, P. Maesschalck, N. Rombaut, R. Sierens, Int. J. Hydrogen Energy **34**(5), 2504 (2009).
- [6] A. Chatzidakis, E. Nikolakaki, S. Sotiropoulos, I. Poulos, Catal. Today **209**, 60 (2013).
- [7] F. M. Ren, W. Hu, Z. F. Zhou, H. H. Ma, W. B. Xu, Optoelectron. Adv. Mat. **8**(9-10), 858 (2014).
- [8] R. Sasikala, V. Sudarsan, C. Sudakar, R. Naik, L. Panicker, S. R. Bharadwaj, Int. J. Hydrogen Energy **34**(15), 6105 (2009).
- [9] E. Filippo, C. Carlucci, A. L. Capodilupo, P. Perulli, F. Conciauro, G. A. Corrente, G. Gigli, G. Ciccarella, Appl. Surf. Sci. **331**, 292 (2015).
- [10] M. Ge, J. Cai, J. Iocozzia, C. Cao, J. Huang, X. Zhang, J. Shen, S. Wang, S. Zhang, K.-Q. Zhang, Y. Lai, Z. Lin, Int. J. Hydrogen Energy **42**(12), 8418 (2017).
- [11] Y. Kameshima, Y. Tamura, A. Nakajima, K. Okada, Appl. Clay. Sci. **45**(1-2), 20 (2009).
- [12] L. J. Guo, L. Zhao, D. W. Jing, Y. J. Lu, H. H. Yang, B. F. Bai, X. M. Zhang, L. J. Ma, X. M. Wu, Energy **34**(9), 1073 (2009).
- [13] Y. Shi, D. Yang, Y. Li, J. Qu, Z.-Z. Yu, Appl. Surf. Sci. **426**, 622 (2017).
- [14] L.-L. Tan, W.-J. Ong, S.-P. Chai, B. T. Goh, A. R. Mohamed, Appl. Catal. B-Environ. **179**, 160 (2015).
- [15] H. Wang, X. Yuan, Y. Wu, G. Zeng, H. Dong, X. Chen, L. Leng, Z. Wu, L. Peng, Appl. Catal. B-Environ. **186**, 19 (2016).
- [16] C. Xing, Z. Wu, D. Jiang, M. Chen, J. Colloid Interf. Sci. **433**, 9 (2014).
- [17] S. Yang, C.-Y. Xu, B.-Y. Zhang, L. Yang, S.-P. Hu, L. Zhen, J. Colloid Interf. Sci. **491**, 230 (2017).
- [18] X. Zhang, X. Li, C. Shao, J. Li, M. Zhang, P. Zhang, K. Wang, N. Lu, Y. Liu, J. Hazard. Mater. **260**, 892 (2013).
- [19] H. Dzinun, M. H. D. Othman, A. F. Ismail, M. H. Puteh, M. A. Rahman, J. Jaafar, J. Wat. Pro Engin. **15**, 78 (2017).

-----  
\*Corresponding author: chfs@cczu.edu.cn